nature immunology

Inhibition of the kinase Csk in thymocytes reveals a requirement for actin remodeling in the initiation of full TCR signaling

Ying Xim Tan[1], Boryana N Manz[1], Tanya S Freedman[1], Chao Zhang[2], Kevan M Shokat[3,4] & Arthur Weiss[1,4,5]

Signaling via the T cell antigen receptor (TCR) is initiated by Src-family kinases (SFKs). To understand how the kinase Csk, a negative regulator of SFKs, controls the basal state and the initiation of TCR signaling, we generated mice that express a Csk variant sensitive to an analog of the common kinase inhibitor PP1 (Csk^{AS}). Inhibition of Csk^{AS} in thymocytes, without engagement of the TCR, induced potent activation of SFKs and proximal TCR signaling up to phospholipase C-γ1 (PLC-γ1). Unexpectedly, increases in inositol phosphates, intracellular calcium and phosphorylation of the kinase Erk were impaired. Altering the actin cytoskeleton pharmacologically or providing costimulation via CD28 'rescued' those defects. Thus, Csk has a critical role in preventing TCR signaling. However, our studies also revealed a requirement for actin remodeling, initiated by costimulation, for full TCR signaling.

Signals transduced by the T cell antigen receptor (TCR) are critical for the selection and maturation of thymocytes and the homeostasis and activation of peripheral T cells, as well as the specification of effector and memory cell fates. Hence, the initiation of TCR signaling in response to antigens of diverse affinities at different stages of T cell development must be tightly regulated. Such regulation ensures the selection of a protective T cell repertoire and the mounting of efficacious immune responses to foreign pathogens while preventing aberrant activation of the immune system. The TCR complex has no intrinsic kinase activity but instead has two spatially separated tyrosine residues in immunoreceptor tyrosine-based activation motifs (ITAMs) located in the cytoplasmic tails of its non–ligand-binding CD3 and ζ-chain subunits[1]. Phosphorylation of those ITAMs is mediated by the T cell Src-family kinase (SFKs) Lck and Fyn T and thereby creates docking sites for recruitment of the cytoplasmic kinase Zap70 via its tandem Src-homology 2 domains. The autoinhibited conformation of Zap70 is relieved by its ITAM binding as well as by the phosphorylation of Zap70 by Lck or Fyn T. Activation of Zap70 is critical for downstream signaling events that lead to cellular responses.

In freshly isolated resting thymocytes and T cells, nonphosphorylated Zap70 is bound to constitutively phosphorylated ζ-chain ITAMs[2]. After prolonged cell culture, the constitutively phosphorylated state of the ITAMs in primary cells is lost but is reinduced by stimulation of the TCR, as it is in T cell lines. Various mechanisms have been proposed for how the phosphorylation of ITAMs and/or Zap70 by SFKs is initiated during stimulation of the TCR. Those include coligation of the coreceptor CD4 or CD8 with the TCR by peptide-bound major histocompatibility complex (pMHC), which redistributes the coreceptor-associated SFK Lck into proximity with TCR ITAM–Zap70; a conformational change in the TCR induced by the binding of pMHC that permits increased accessibility of ITAMs to SFKs; and redistribution of bulky transmembrane phosphatases that inhibit signaling away from the narrow TCR-pMHC cell-cell interface due to size exclusion (i.e., the kinetic-segregation model)[3–5]. The relative importance of such mechanisms has remained unresolved because the experimental evidence available is conflicting or incomplete. It is also uncertain if any of those mechanisms alone is sufficient to trigger full downstream TCR signaling.

Since SFKs phosphorylate TCR ITAMs, the control of their activities represents a key regulatory node in the initiation of TCR signaling. Trans-autophosphorylation of a conserved activation-loop tyrosine in the SFK catalytic domain increases catalytic activity[6]. Phosphorylation of the conserved carboxy-terminal inhibitory tyrosine of SFKs by the tyrosine kinase Csk promotes their closed, inactive conformation[7]. In T cells, the receptor-like tyrosine phosphatase CD45 opposes the action of Csk and dephosphorylates the inhibitory tyrosine. Thus, the equilibrium between Csk and CD45 may set the threshold for the activation of TCR signaling[8]. In resting T cells, there are various phosphorylation states of Lck: unphosphorylated, each of the singly phosphorylated species and the doubly phosphorylated species[9]. It is unclear if that basal equilibrium has a fixed state or is a dynamic, ongoing process in unstimulated primary T cells.

Csk is a ubiquitously expressed, cytosolic protein. Since Csk-deficient mice die *in utero* due to excessive SFK activity, and conditional

[1]Rosalind Russell–Ephraim P. Engleman Medical Research Center for Arthritis, Division of Rheumatology, Department of Medicine, University of California, San Francisco, California, USA. [2]Department of Chemistry, University of Southern California, California, USA. [3]Department of Cellular and Molecular Pharmacology, University of California, San Francisco, California, USA. [4]Howard Hughes Medical Institute, Chevy Chase, Maryland, USA. [5]Department of Microbiology and Immunology, University of California, San Francisco, California, USA. Correspondence should be addressed to A.W. (aweiss@medicine.ucsf.edu).

Received 16 September; accepted 23 October; published online 8 December 2013; doi:10.1038/ni.2772

deletion of Csk in thymocytes results in TCR- and MHC-independent development of abnormal CD4$^+$ T cells, understanding the importance of regulating Csk in the T cell lineage has been challenging[10–12]. The positioning of Csk at the plasma membrane, proximal to the membrane-localized SFKs, is thought to be regulated through protein-protein interactions that may mediate its dynamic translocation between the cytosol and the cell membrane[13]. The lipid raft–localized transmembrane adaptor PAG is believed to be involved in the recruitment of Csk to lipid rafts, where some SFK molecules are located and initiation of TCR signaling may occur[14–17]. However, in contrast to Csk-deficient mice, PAG-deficient mice develop normally without defect in T cell development or signaling, which indicates the existence of alternative mechanisms for regulating Csk[18,19].

To investigate the role of Csk activity in TCR signaling, we generated a novel allele of *Csk* (*Csk*^{AS}) by mutating the residue encoding the conserved bulky gatekeeper amino acid in its ATP-binding pocket, thereby enlarging the pocket. The kinase activity of the resultant mutant Csk^{AS} protein is specifically and rapidly inhibited by 3-iodo-benzyl-PP1 (3-IB-PP1), a bulky analog of the common kinase inhibitor PP1. Unexpectedly, in Jurkat human T lymphocytes, inhibiting the kinase activity of a dominant inhibitory membrane-targeted Csk^{AS} induces potent activation of SFKs and ligand-independent TCR signaling[20]. That finding suggests that perturbing the finely tuned Csk-CD45 kinase-phosphatase activity equilibrium can lead to activation of SFKs and trigger initiation of TCR signaling. However, Jurkat T cells endogenously express Csk, so the expression of membrane-targeted Csk^{AS} may have induced compensatory 'rewiring' of the signaling circuitry or activation could have reflected a dominant-negative effect mediated by the protein-interaction domains of the inhibited Csk^{AS}.

To determine the role of Csk in controlling the basal state and initiation of TCR signaling in primary T lineage cells, we generated mice that express only the normally regulated, cytosolic form of Csk^{AS}. We found that inhibition of Csk^{AS} alone in thymocytes led to strong activation of SFKs and proximal signaling but did not result in full downstream TCR signaling in the absence of additional remodeling of the actin cytoskeleton. Our data suggested a major role for Csk in restraining SFK activation in the basal state and that SFK activation alone was sufficient for the initiation of proximal TCR signaling. However, our studies also indicated that in addition to SFK activity, the actin cytoskeleton must be remodeled in thymocytes for downstream signal propagation. That requisite remodeling of the cytoskeleton was most probably mediated by costimulation via CD28.

RESULTS

Generation of Csk^{AS} mice

We introduced *Csk*^{AS} into mice by bacterial artificial chromosome (BAC) transgenesis. The Csk^{AS} protein was 25% as active as wild-type Csk (**Supplementary Fig. 1a**,**b**). We obtained three independent founders and crossed them with *Csk*$^{+/-}$ mice, ultimately removing expression of endogenous wild-type *Csk*. Two of the lines expressed less than 50% of the Csk expressed by wild-type mice and displayed defects in T cell development (data not shown). The third line had approximately 2.5-fold as much expression of Csk as wild-type mice had but displayed normal T cell development (**Supplementary Fig. 2a–c**). Notably, the TCR responses of Csk^{AS} thymocytes to stimulation with high or low doses of monoclonal antibody to CD3ε (anti-CD3ε) were similar to those of wild-type thymocytes (**Supplementary Fig. 2d**). We therefore used that third Csk^{AS} line for further studies.

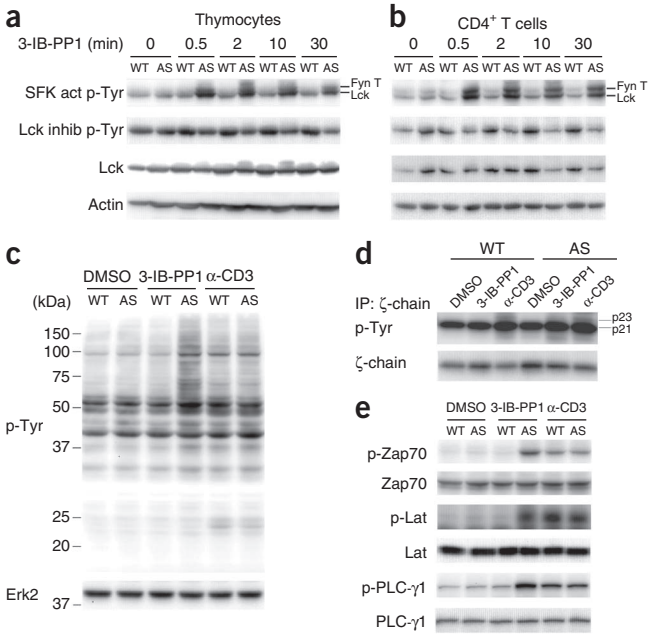

Figure 1 Inhibition of Csk^{AS} in primary mouse T cells induces hyperactivation of SFKs and phosphorylation of TCR-proximal signaling molecules. (**a**,**b**) Immunoblot analysis of phosphorylation of the activation-loop tyrosine of Lck and Fyn T (SFK act p-Tyr) and the inhibitory tyrosine of Lck (Lck inhib p-Tyr), as well as total Lck and actin (loading control), in wild-type (WT) or Csk^{AS} (AS) thymocytes (**a**) or peripheral CD4$^+$ T cells (**b**) treated for 0–30 min (above lanes) with 10 μM 3-IB-PP1. (**c**) Immunoblot analysis of phosphorylated tyrosine (p-Tyr) and Erk2 (loading control) in wild-type or Csk^{AS} thymocytes treated for 3 min with vehicle (DMSO), 10 μM 3-IB-PP1 or 20 μg/ml anti-CD3ε (α-CD3ε). Left margin, molecular size in kilodaltons (kDa). (**d**) Immunoblot analysis of phosphorylated tyrosine and ζ-chain in wild-type or Csk^{AS} thymocytes treated for 3 min with vehicle, 10 μM 3-IB-PP1 or 20 μg/ml anti-CD3ε and then lysed, followed by immunoprecipitation with anti-ζ. (**e**) Immunoblot analysis of total and phosphorylated (p-) Zap70, Lat and PLC-γ1 in wild-type or Csk^{AS} thymocytes treated for 3 min with vehicle, 10 μM 3-IB-PP1 or 20 μg/ml anti-CD3ε. Data are representative of three independent experiments.

Inhibiting Csk^{AS} activates SFKs and proximal TCR signaling

At a dose of 10 μM, 3-IB-PP1 strongly inhibited recombinant Csk^{AS} but not wild-type Csk (**Supplementary Fig. 1c**,**d**). Treatment of thymocytes or peripheral CD4$^+$ T cells with 3-IB-PP1 rapidly led to sustained hyperphosphorylation of the activation-loop tyrosine of both Lck and Fyn T, as well as slower progressive dephosphorylation of the inhibitory tyrosine of Lck, in Csk^{AS} cells but not in wild-type cells (**Fig. 1a**,**b**). These data reconfirmed the role of Csk as the main negative regulator of SFKs. The findings also indicated that in mouse T cells, the basal phosphorylation status of Lck was in a dynamic equilibrium that required constant restraint by Csk activity. Removal of that constraint drove rapid ligand-independent autoactivation of SFKs, presumably by trans-autophosphorylation. The incomplete dephosphorylation of the inhibitory tyrosine of Lck may indicate that a subset of Lck molecules is shielded from or is inaccessible to the phosphatase activity of CD45.

The activation of Lck could lead to initiation of TCR signaling. Lck phosphorylates CD3 and ζ-chain ITAMs in the TCR, which allows the recruitment, phosphorylation and activation of Zap70. Active Zap70 phosphorylates Lat and SLP-76, which form a supramolecular signalosome that recruits the phospholipase PLC-γ1. Subsequent

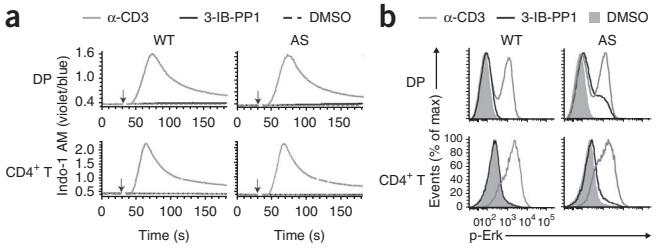

Figure 2 Increases in intracellular Ca^{2+} and Erk phosphorylation are impaired following inhibition of Csk^{AS}. (**a**) Change in Ca^{2+} in wild-type or Csk^{AS} $CD4^+CD8^+$ thymocytes (DP) or purified peripheral $CD4^+$ T cells ($CD4^+$ T) loaded with the Ca^{2+} indicator Indo-1 AM and stimulated (downward arrows) with vehicle (DMSO), 10 μM 3-IB-PP1 or 20 μg/ml anti-CD3ε, presented as the ratio of violet fluorescence intensity to blue fluorescence intensity (violet/blue). (**b**) Phosphorylated Erk (p-Erk) in wild-type or Csk^{AS} thymocytes or splenocytes stimulated for 2 min as in **a**, gated on $CD4^+CD8^+$ thymocytes (DP) or $CD4^+$ splenocytes ($CD4^+$ T). Data are representative of three independent experiments.

phosphorylation of PLC-γ1 on Tyr783 by kinases of the Tec family leads to its activation and the hydrolysis of phosphatidylinositol-(4,5)-bisphosphate ($PtdIns(4,5)P_2$)[1]. The class I phosphatidylinositol-3-OH kinase-δ (PI(3)K-δ) is also activated after stimulation of the TCR and phosphorylates $PtdIns(4,5)P_2$ to phosphatidylinositol-(3,4,5)-trisphosphate ($PtdIns(3,4,5)P_3$), which regulates phosphorylation of the kinase Akt[21]. In thymocytes, activation of Lck in response to inhibition of Csk^{AS} led to increased global tyrosine phosphorylation, including phosphorylation of the ζ-chain to its fully phosphorylated form (p23) (**Fig. 1c**,**d** and **Supplementary Fig. 3a**). Inhibition of Csk^{AS} also induced phosphorylation of Zap70, Lat, PLC-γ1 and Akt in thymocytes similar to the phosphorylation that resulted from crosslinking of CD3 (**Fig. 1e** and **Supplementary Fig. 3b**). The phosphorylation of both PLC-γ1 and Akt was consistent with the activation of Tec kinases in response to Csk inhibition. Overall, our data indicated that inhibiting Csk increased the activation of SFKs, which led to the proximal phosphorylation events associated with TCR signaling even without engagement of the receptor. In contrast to the conformational-change and kinetic-segregation models of TCR triggering, our findings suggested that by activating SFKs, proximal signaling could be initiated even without inducing a conformational change in the TCR or segregating the TCR from abundant large transmembrane phosphatases such as CD45.

Impaired downstream signaling after inhibition of Csk^{AS}

Active PLC-γ1 hydrolyzes $PtdIns(4,5)P_2$ into diacylglycerol and inositol-(1,4,5)-trisphosphate ($Ins(1,4,5)P_3$), which activate the signaling pathways of the GTPase Ras and kinase Erk and of calcium (Ca^{2+}), respectively[1]. Unexpectedly, in contrast to stimulation of the TCR with anti-CD3, the inhibition of Csk^{AS} that led to similar increases in the phosphorylation of PLC-γ1 in thymocytes was not associated with increased intracellular Ca^{2+} or robust phosphorylation of Erk (**Fig. 2a**,**b**). The limited phosphorylation of Erk seen in DP thymocytes was not sufficient to drive upregulation of expression of the activation marker CD69 (**Supplementary Fig. 3c**). The defect in Erk phosphorylation was more severe in peripheral $CD4^+$ T cells than in DP thymocytes, and this correlated with less phosphorylation of Zap70, Lat and PLC-γ1 than that obtained by crosslinking of CD3 (**Fig. 2a**,**b** and **Supplementary Fig. 3d**,**e**).

$Ins(1,4,5)P_3$ is rapidly metabolized to inositol-(1,4)-bisphosphate and inositol-(1)-phosphate[22]. Therefore, measuring total production of inositol phosphates in the presence of lithium chloride, an inhibitor of inositol-(1)-phosphate phosphatase, reflects overall hydrolysis of $PtdIns(4,5)P_2$ by PLC-γ1. We found that total production of inositol phosphates in thymocytes was much lower after inhibition of Csk^{AS} than after stimulation of the TCR (**Fig. 3a**). The small increase in total inositol phosphates probably correlated with a small amount

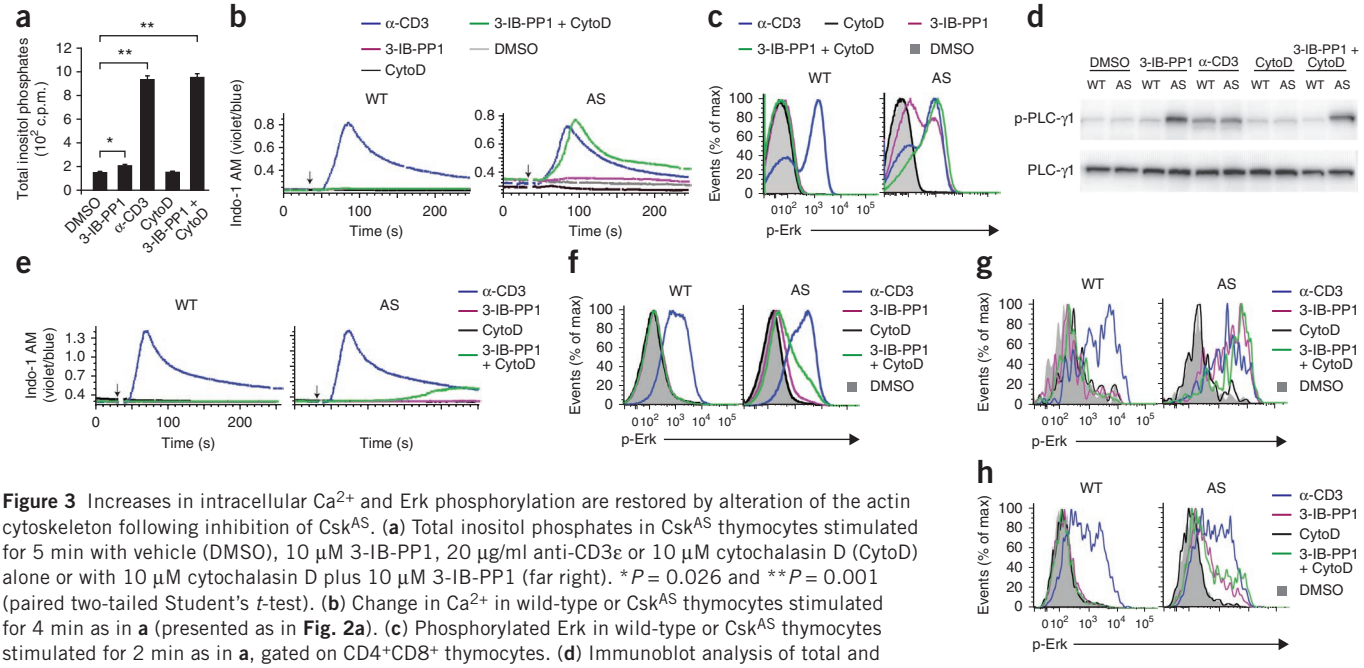

Figure 3 Increases in intracellular Ca^{2+} and Erk phosphorylation are restored by alteration of the actin cytoskeleton following inhibition of Csk^{AS}. (**a**) Total inositol phosphates in Csk^{AS} thymocytes stimulated for 5 min with vehicle (DMSO), 10 μM 3-IB-PP1, 20 μg/ml anti-CD3ε or 10 μM cytochalasin D (CytoD) alone or with 10 μM cytochalasin D plus 10 μM 3-IB-PP1 (far right). $*P = 0.026$ and $**P = 0.001$ (paired two-tailed Student's *t*-test). (**b**) Change in Ca^{2+} in wild-type or Csk^{AS} thymocytes stimulated for 4 min as in **a** (presented as in **Fig. 2a**). (**c**) Phosphorylated Erk in wild-type or Csk^{AS} thymocytes stimulated for 2 min as in **a**, gated on $CD4^+CD8^+$ thymocytes. (**d**) Immunoblot analysis of total and phosphorylated PLC-γ1 in wild-type or Csk^{AS} thymocytes treated for 3 min as in **a**. (**e**) Change in Ca^{2+} in wild-type or Csk^{AS} $CD4^+$ splenocytes stimulated as in **a** (presented as in **Fig. 2a**). (**f**) Phosphorylated Erk in wild-type or Csk^{AS} splenocytes stimulated for 2 min as in **a**, gated on $CD4^+$ splenocytes. (**g**,**h**) Phosphorylated Erk in wild-type or Csk^{AS} thymocytes (**g**) or purified T cells (**h**) stimulated for 2 min as in **a**, gated on $CD4^-CD8^-$ γδ TCR^+ cells. Data are representative of three independent experiments (mean and s.e.m. of technical replicates in **a**).

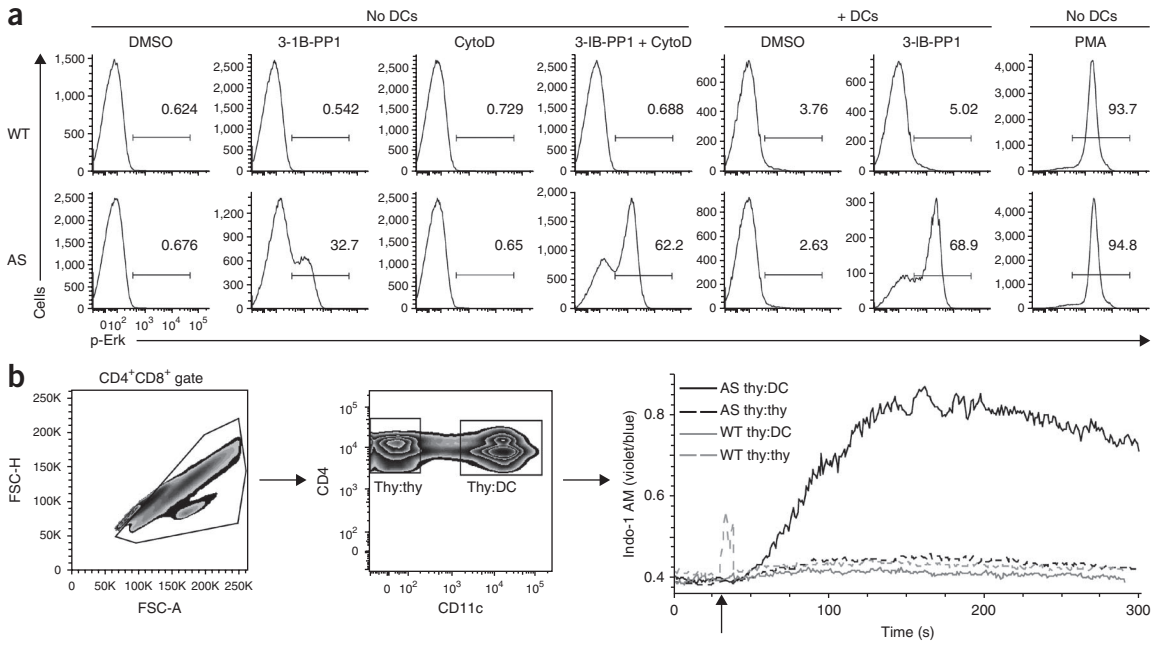

Figure 4 Mature DCs restore the Ca^{2+} increase and Erk phosphorylation following inhibition of Csk^{AS}. (**a**) Phosphorylated Erk in wild-type or Csk^{AS} thymocytes pelleted with (+ DCs) or without (No DCs) activated DCs (enriched from wild-type splenocytes and activated by overnight culture) at a ratio of 1:1 and stimulated for 3 min with vehicle (DMSO), 10 μM 3-IB-PP1 or 10 μM cytochalasin D (alone or with 10 μM 3-IB-PP1) or with 50 ng/ml phorbol myristate acetate (PMA), gated on $CD4^+CD8^+$ thymocytes. Numbers above bracketed lines indicate percent cells with phosphorylated Erk. (**b**) Change in Ca^{2+} (right; as in **Fig. 2a**) in wild-type or Csk^{AS} thymocytes loaded with Indo-1 AM and stained on the surface for CD4 and CD8, then mixed at a ratio of 1:1 with activated DCs (prepared as in **a** and stained on the surface for CD11c) and stimulated (upward arrow) for 5 min with 10 μM 3-IB-PP1, gated for $CD4^+CD8^+$ multiplets (left), then further separated (middle) into thymocyte-thymocyte conjugates (thy:thy; $CD11c^-$) and thymocyte-DC conjugates (thy:DC; $CD11c^+$). FSC, forward scatter (-H, height; -A, area). Data are representative of three independent experiments.

of diacylglycerol that may have been sufficient to activate the Ras guanine-exchange factor RasGRP1 but may not have generated enough Ras-GTP to drive the positive feedback loop for Ras activation by SOS, a Ras guanine-exchange factor that is allosterically activated by Ras-GTP. Such a small increase in diacylglcerol may have accounted for the very small amount of Erk phosphorylation we observed. Alternatively, a PLC-γ1-independent RasGRP1-Erk pathway may be involved[23].

Alteration of the actin cytoskeleton restores full TCR signaling

The cortical actin cytoskeleton restricts the lateral diffusion of transmembrane molecules[24], and actin-binding proteins can sequester $PtdIns(4,5)P_2$ (refs. 25,26). Altering the actin cytoskeleton alone in primary B cells can activate calcium and Erk pathways[27]. We speculated that the cortical actin cytoskeleton might limit the PLC-γ1 activity induced downstream of Csk^{AS} inhibition. Indeed, Csk^{AS} thymocytes treated simultaneously with 3-IB-PP1 and the actin-modifying agent cytochalasin D had increased total inositol phosphates, intracellular Ca^{2+} and Erk phosphorylation comparable to that obtained by crosslinking of CD3 (**Fig. 3a–c**). In contrast, treatment of Csk^{AS} thymocytes with cytochalasin D alone did not result in an increase in intracellular Ca^{2+} or Erk phosphorylation. We observed similar responses to other actin-modifying agents (**Supplementary Fig. 4**). The increase in hydrolysis of $PtdIns(4,5)P_2$ and downstream responses induced by altering the actin cytoskeleton was not accounted for by changes in the phosphorylation of PLC-γ1 (**Fig. 3d**). These data suggested that remodeling of the actin cytoskeleton had a crucial role in downstream TCR signaling events in thymocytes by controlling the access of PLC-γ1 to $PtdIns(4,5)P_2$. In contrast, phosphorylation of Akt was induced by inhibition of Csk^{AS} alone, which indicated that the access of PI(3)K to $PtdIns(4,5)P_2$ and the access of Akt to $PtdIns(3,4,5)P_3$ were not regulated as strongly by the actin cytoskeleton.

Altering the actin cytoskeleton in peripheral $CD4^+$ T cells, however, only partially 'rescued' the defect in intracellular Ca^{2+} increase and Erk phosphorylation after inhibition of Csk^{AS} (**Fig. 3e,f**). Given our earlier observation that proximal phosphorylation induced by inhibition of Csk^{AS} in peripheral $CD4^+$ T cells was impaired (**Supplementary Fig. 3e**), it seemed that additional regulatory mechanisms for signal initiation developed in more mature T cells. In support of that possibility, we found that although inhibition of Csk^{AS} alone induced substantial phosphorylation of Erk in immature thymic γδ T cells, that responsiveness was greatly reduced in mature splenic γδ T cells, which acted like peripheral $CD4^+$ T cells (**Fig. 3g,h**). Thus, altering the actin cytoskeleton 'rescued' the defect in full downstream signaling via calcium and Ras-Erk after inhibition of Csk^{AS} in immature thymocytes but not in mature peripheral T cells.

Mature dendritic cells restore full TCR signaling

We sought to determine if there was a physiological costimulus that could induce the requisite remodeling of the cytoskeleton in thymocytes that was not achieved in response to the activation of SFKs by inhibition of Csk^{AS} alone. *In vivo*, thymocytes initiate TCR signaling when they recognize pMHC molecules on antigen-presenting cells (APCs) such as thymic epithelial cells or dendritic cells (DCs). APCs also express many costimulatory molecules that can provide additional signals. The TCR signal together with costimulatory signals dictate thymocyte developmental fate[28]. Notably, the interaction of

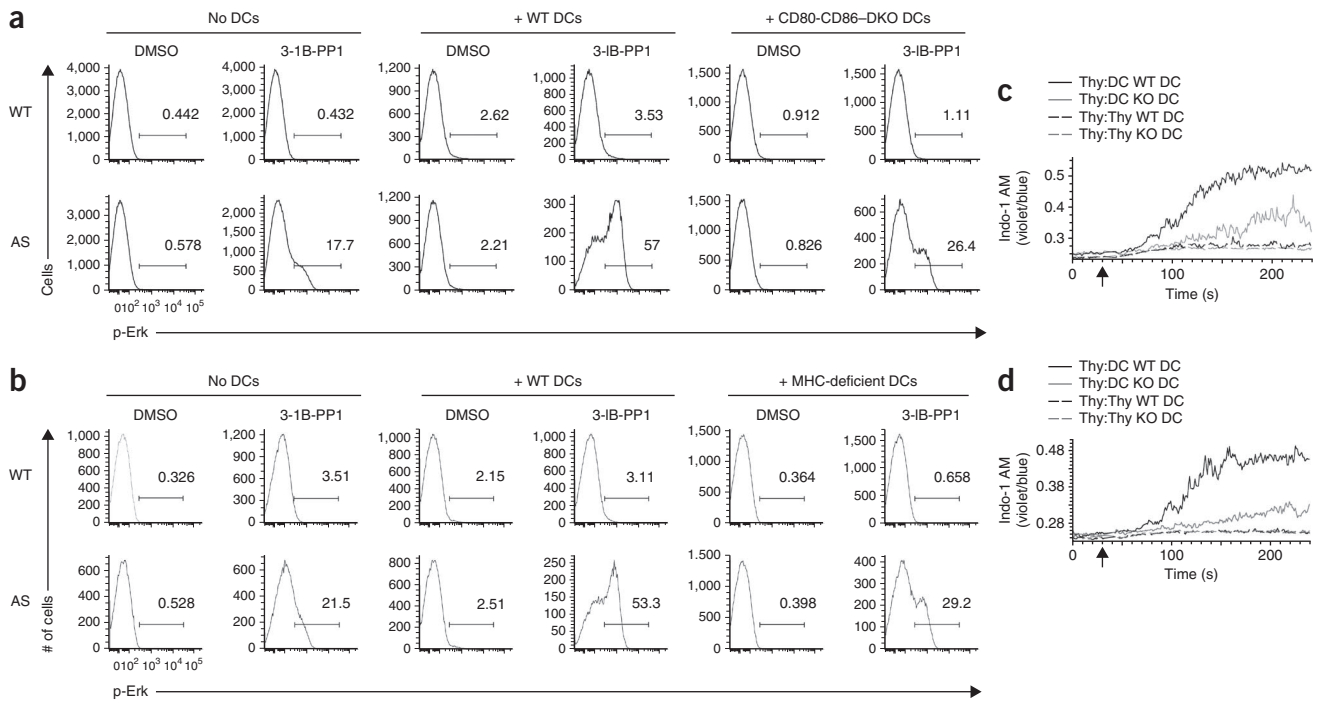

Figure 5 Restoration of full TCR signaling after inhibition of Csk^{AS} requires both MHC and the CD28 ligands CD80 and CD86 on DCs. (**a**,**b**) Phosphorylated Erk in wild-type or Csk^{AS} thymocytes pelleted with or without activated DCs (enriched from wild-type splenocytes or splenocytes doubly deficient in CD80 and CD86 (CD80-CD86–DKO; **a**) or MHC class I and class II (MHC-KO; **b**) and activated by overnight culture) at a ratio of 1:1 and stimulated for 3 min with vehicle (DMSO) or 10 μM 3-IB-PP1, gated on CD4$^+$CD8$^+$ thymocytes. Numbers above bracketed lines indicate percent cells with phosphorylated Erk. (**c**,**d**) Change in Ca^{2+} (right; as in **Fig. 2a**) in wild-type or Csk^{AS} thymocytes loaded with Indo-1 AM and stained on the surface for CD4 and CD8, then mixed at a ratio of 1:1 with activated DCs doubly deficient in CD80 and CD86 (**c**) or MHC class I and class II (**d**) (prepared as in **a** and stained on the surface for CD11c) and stimulated with 10 μM 3-IB-PP1 (gated and separated as in **Fig. 4b**). Data are representative of three independent experiments.

polyclonal thymocytes with activated splenic DCs, in thymocyte-DC conjugates, enhanced Erk phosphorylation and increased intracellular Ca^{2+} in Csk^{AS} thymocytes when Csk^{AS} was inhibited, but similar interaction with naive splenic DCs did not (**Fig. 4** and **Supplementary Fig. 5a**). As splenic DCs activated *in vitro* may differ from thymic DCs[29], which are the physiological APCs for thymocytes, we assessed the ability of thymic DCs to enhance the phosphorylation of Erk induced by inhibition of Csk^{AS}. Thymic DCs did enhance the activation of Erk in Csk^{AS} cells treated with 3-IB-PP1, albeit to a lesser extent than when we used mature splenic DCs (**Supplementary Fig. 5b**). Overall, our findings demonstrated that mature DCs were able to restore full TCR signaling after inhibition of Csk^{AS}.

MHC and costimulatory proteins needed for full signaling

We postulated that DCs restored full activation of TCR signaling, leading to an increase in intracellular Ca^{2+} and activation of Erk in response to inhibition of Csk^{AS} by providing a costimulatory signal that initiated remodeling of the actin cytoskeleton. Through the use of a 'candidate' approach, we assessed the role of several pathways known to influence actin remodeling during T cell–APC interactions[30]. The diminished ability of activated DCs doubly deficient in the costimulatory molecules CD80 and CD86 to enhance 3-IB-PP1-induced phosphorylation of Erk indicated the importance of their coreceptor, CD28 (**Fig. 5a**). In contrast, activated DCs deficient in the adhesion molecule ICAM-1 enhanced 3-IB-PP1-induced phosphorylation of Erk as potently as activated wild-type DCs did (**Supplementary Fig. 5c**), which suggested that the T cell integrin LFA-1 (CD58; $\alpha_L\beta_2$) was dispensable in this process. Likewise, inhibition of signaling via G_i protein–coupled receptors in thymocytes with pertussis toxin had no effect (**Supplementary Fig. 5d**), which challenged the possibility that chemokine receptors were involved in this. Most Lck in thymocytes is associated with the coreceptor CD4 or CD8, which dock with MHC and thus recruit coreceptor-bound Lck to the TCR[31]. We found that activated DCs doubly deficient in MHC class I and MHC class II had diminished ability to enhance the phosphorylation of Erk after treatment with 3-IB-PP1 (**Fig. 5b**). Similarly, we observed that activated DCs doubly deficient in CD80 and CD86 or in MHC class I and MHC class II had reduced ability to induce an increase in intracellular Ca^{2+} in Csk^{AS} thymocytes treated with 3-IB-PP1 (**Fig. 5c**,**d**). Thus, our data revealed that activated DCs required expression of CD28 counter-ligands and MHC to restore full TCR signaling in thymocytes, which led to calcium and Erk responses when Csk^{AS} was inhibited. That finding was consistent with our observation that naive DCs were unable to restore full TCR signaling (**Supplementary Fig. 5a**), as expression of CD80, CD86 and MHC is upregulated during DC maturation[32].

CD28 engagement restores robust Erk phosphorylation

We next determined whether providing the CD28-CD86 interaction alone would be sufficient to enhance the phosphorylation of Erk after inhibition of Csk^{AS}. Indeed, inhibition of Csk^{AS} in thymocytes in the presence of beads coated with a CD86-immunoglobulin fusion protein increased Erk phosphorylation (**Fig. 6a**). Moreover, coating the beads with both CD86-immunoglobulin and MHC class II tetramer further increased the extent of Erk phosphorylation, even though MHC class II tetramer alone did not increase Erk phosphorylation (**Fig. 6a**). These results provided evidence that CD28-CD86–induced signals were sufficient

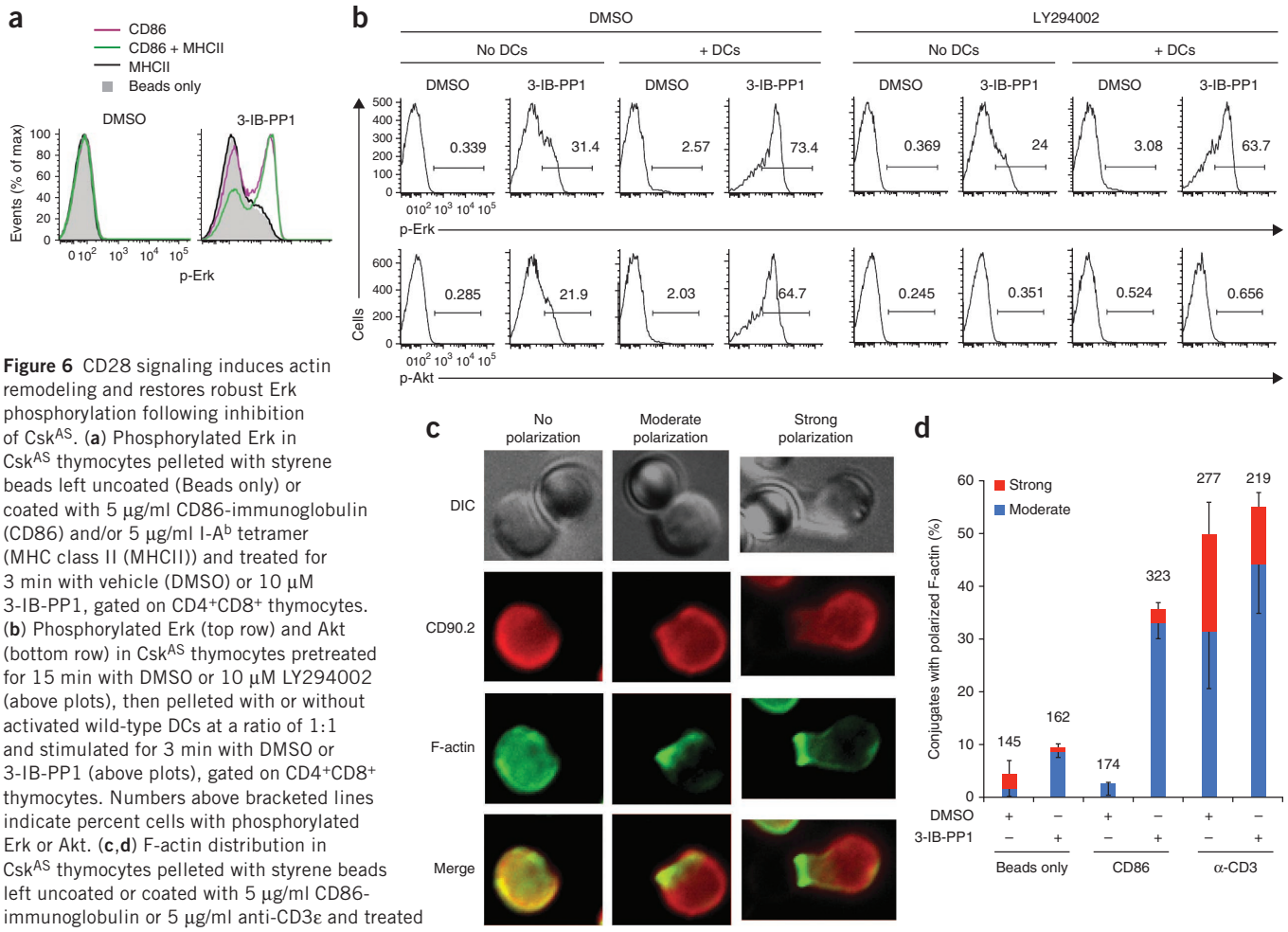

Figure 6 CD28 signaling induces actin remodeling and restores robust Erk phosphorylation following inhibition of Csk^{AS}. (**a**) Phosphorylated Erk in Csk^{AS} thymocytes pelleted with styrene beads left uncoated (Beads only) or coated with 5 μg/ml CD86-immunoglobulin (CD86) and/or 5 μg/ml I-A^{b} tetramer (MHC class II (MHCII)) and treated for 3 min with vehicle (DMSO) or 10 μM 3-IB-PP1, gated on CD4^{+}CD8^{+} thymocytes. (**b**) Phosphorylated Erk (top row) and Akt (bottom row) in Csk^{AS} thymocytes pretreated for 15 min with DMSO or 10 μM LY294002 (above plots), then pelleted with or without activated wild-type DCs at a ratio of 1:1 and stimulated for 3 min with DMSO or 3-IB-PP1 (above plots), gated on CD4^{+}CD8^{+} thymocytes. Numbers above bracketed lines indicate percent cells with phosphorylated Erk or Akt. (**c**,**d**) F-actin distribution in Csk^{AS} thymocytes pelleted with styrene beads left uncoated or coated with 5 μg/ml CD86-immunoglobulin or 5 μg/ml anti-CD3ε and treated for 3 min with vehicle (DMSO) or 10 μM 3-IB-PP1, then stained for CD90.2 and F-actin (in **c**), presented as the distribution patterns observed under all conditions (**c**) and frequency of conjugates with moderate (– s.e.m.) or strong (+ s.e.m.) F-actin polarization at the bead-thymocyte interface (**d**). DIC, differential interference contrast. Original magnification (**c**), ×40. Numbers above bars (**d**) indicate total conjugates analyzed. Data are representative of three independent experiments (mean and s.e.m. in **d**).

to restore robust Erk signaling after inhibition of Csk^{AS}, particularly when MHC-mediated interactions were also present.

CD28 engagement induces actin remodeling

We hypothesized that the CD28-mediated costimulation provided by activated DCs restored robust Erk activation by inducing actin remodeling in thymocytes. CD28 signaling has been shown to induce both PI(3)K activation and actin remodeling[33,34]. The Tyr-Met-Asn-Met (YMNM) motif in the cytoplasmic tail of CD28 recruits the p85 subunit of PI(3)K. In addition, the actin-cytoskeletal regulators Vav-1, cofilin-1 and Rltpr are activated downstream of CD28 (ref. 35). To determine if PI(3)K signaling has a role in the restoration of full TCR signaling by activated DCs, we pretreated thymocytes with the PI(3)K inhibitor LY294002 before inhibiting Csk^{AS} in the presence of activated DCs. We found that although Akt phosphorylation was completely abrogated, as expected, the enhancement in Erk phosphorylation was unaffected (**Fig. 6b**), which suggested that PI(3)K signaling was not important for this effect.

We then explored the role of CD28 signaling in actin remodeling by imaging the distribution of F-actin of thymocytes conjugated to beads coated with CD86-immunoglobulin and treated with 3-IB-PP1. We observed polarization of F-actin and its accumulation at the interface of thymocytes and the beads coated with CD86-immunoglobulin when Csk^{AS} was inhibited (**Fig. 6c**,**d**). In contrast, 3-IB-PP1 alone induced only a negligible amount of F-actin polarization (**Fig. 6c**,**d**), which indicated that this actin remodeling required both CD28 engagement and SFK activation. In conclusion, our data support the following model: after activation of SFKs, actin remodeling, which can be induced by engagement of CD28, allows the hydrolysis of PtdIns(4,5)P_2 by active PLC-γ1, resulting in the downstream propagation of full TCR signaling in thymocytes (**Supplementary Fig. 6**).

DISCUSSION

In this study, we generated mice that express Csk^{AS}, which allowed genetically specific and rapid inhibition of the kinase activity of Csk in cells. This enabled us to elucidate the function of that kinase activity in the initiation of TCR signaling in unmanipulated primary T cells. After inhibition of Csk^{AS} in thymocytes, we observed rapid hyperactivation of Lck and Fyn T, which in turn induced the phosphorylation of proximal TCR signaling components up to and including PLC-γ1. We propose that a dynamic equilibrium of Csk and CD45 activity controls SFK activity and is responsible for maintaining the basal unstimulated state of the most proximal components of the TCR signaling pathway. Such an ongoing equilibrium may confer rapid plasticity to the Lck-activation status and allow sensitive and

efficient TCR triggering in response to receptor engagement. Our results also suggested that Csk has the dominant inhibitory role in controlling the basal state and may be largely responsible for setting the threshold for TCR signaling. Inhibition of Csk function without perturbation of CD45 or induction of a conformational change in TCR-CD3 can therefore have a prominent physiological role in allowing SFKs to be activated and initiate downstream TCR-dependent signaling. Physiologically, local changes induced by ligating the TCR can be envisioned as influencing this equilibrium through various mechanisms that might influence the localization of Csk, CD45 or Lck (or Fyn T). ITAM accessibility seems to be less of a concern, as the ζ-chain is already largely constitutively phosphorylated *in vivo* in the basal state, although there is a modest increase in its phosphorylation following receptor stimulation.

Notably, our results also suggested that activation of SFK activity alone was insufficient to initiate the full downstream signaling pathway leading to calcium and Erk responses, events critical for cellular activation. In thymocytes, downstream pathway activation requires events that lead to remodeling of the actin cytoskeleton to allow PLC-γ1 access to PtdIns(4,5)P_2. Thus, the actin cytoskeleton can provide a barrier to control the transmission of downstream signaling events. The actin remodeling needed to overcome that barrier may be accomplished experimentally *ex vivo* by ligation of the TCR with very high concentrations of monoclonal antibodies and pMHC complexes. Under physiological conditions in which TCR stimuli are limiting, the function of other coreceptors or costimulatory molecules (such as CD28) that influence remodeling of the actin cytoskeleton is probably necessary for PLC-γ1 to access its substrate.

The requirement for actin remodeling in primary thymocytes to initiate full TCR signaling is in contrast to published findings obtained with Jurkat T cells. Inhibiting Csk in Jurkat T cells, in the absence of TCR engagement and additional manipulation of the actin cytoskeleton, results in substantial increases in intracellular Ca^{2+}, Erk phosphorylation and upregulation of CD69 expression[20]. One reason for that may be that the dynamics of the cortical actin cytoskeleton are different in Jurkat T cells and primary T cells. Jurkat T cells lack expression of the phosphatases PTEN and SHIP-1 that dephosphorylate PtdIns(3,4,5)P_3 and most probably have an abnormal phosphoinositide composition in their plasma membrane[36]. That could in turn have a profound effect on their cortical actin cytoskeleton, since PtdIns(4,5)P_2 and PtdIns(3,4,5)P_3 regulate the assembly of F-actin in cells by binding and influencing the activity of various actin-regulatory proteins[37].

Another notable difference we observed in response to Csk inhibition was between thymocytes and mature $CD4^+$ T cells. Similar to thymocytes, mature $CD4^+$ T cells displayed strong SFK activation after treatment with 3-IB-PP1, but in contrast to thymocytes, the phosphorylation of Zap70, Lat and PLC-γ1 was lower than that achieved by crosslinking with anti-CD3. Furthermore, altering the actin cytoskeleton in mature $CD4^+$ T cells only partially restored the signaling via calcium and Ras-Erk after inhibition of Csk^{AS}. We observed similar differences between immature thymic γδ T cells and mature splenic γδ T cells in their response to inhibition of Csk^{AS}. There are probably additional negative regulatory pathway acquired during development that perhaps involve phosphatases or inhibitory receptors and must be overcome in mature T cells. Alternatively, mature T cells may have different regulatory mechanisms that govern their cortical actin cytoskeletons. Notably, thymic γδ T cells were able to phosphorylate Erk robustly without the need for an additional actin-remodeling stimulus after inhibition of Csk^{AS}, which further underscored the fact that different T cell subsets have distinct regulation of their signal-transduction pathways, most probably due to differences in the 'wiring' of their signaling networks.

The dynamics of the actin cytoskeleton have multiple important roles in T cell activation and have been best studied in the context of the immunological synapse, a supramolecular structure found at the contact site between a T cell and an APC; the synapse is proposed to be important for prolonging and modulating TCR signaling. F-actin first accumulates in the T cell–APC interface, followed by central clearing. Disruption of the actin cytoskeleton with cytochalasin D impairs the formation of TCR microclusters and the immunological synapse[30]. Many pathways downstream of the TCR or costimulatory receptors that are involved in actin remodeling and are important for formation of the immunological synapse have been identified. However, exactly how actin dynamics influence TCR signaling remains elusive. Stimulating cytochalasin D–treated T cells with superantigen-pulsed APCs leads to less calcium flux, but stimulating the same T cells with anti-CD3 leads to prolonged calcium flux[38]. Our results revealed a previously unappreciated direct role for dynamics of the actin cytoskeleton in the initiation of signaling via calcium and Ras-Erk in thymocytes.

A published report has demonstrated that merely altering the actin cytoskeleton in primary naive B cells results in a spontaneous increase in intracellular Ca^{2+} that is dependent on antigen receptor signaling[27]. The hypothesis proposed suggests that in B cells, remodeling of the actin cytoskeleton allows greater mobility of the B cell antigen receptor and increases interactions of that receptor with downstream signaling molecules such as CD19 (ref. 27). In contrast, in primary thymocytes, we have shown that altering the actin cytoskeleton alone did not initiate any TCR signaling events and that additional activation of SFKs was required for full TCR signaling. That difference between T cells and B cells may reflect their differing dependence on basal signaling for peripheral homeostasis and suggests that the initiation of TCR signaling is more tightly regulated than is BCR signaling in B cells[39,40]. Since SFK activation alone was sufficient to induce proximal phosphorylation events in thymocytes, it appears that the predominant role of the cortical actin cytoskeleton in thymocytes is in regulating the access of PLC-γ1 to PtdIns(4,5)P_2.

Lending physiological importance to our finding that remodeling of the actin cytoskeleton was required for full TCR signaling was our observation that activated DCs were able to restore signaling via calcium- and Ras-Erk-dependent pathways after inhibition of Csk^{AS} in thymocytes. That required the presence of CD80 or CD86 on the DCs. Indeed, providing costimulation via CD28 alone during inhibition of Csk^{AS} was sufficient to enhance the phosphorylation of Erk. CD28 signaling induces pathways that include activation of PI(3)K and remodeling of the actin cytoskeleton[33]. Our results demonstrated that the CD28-dependent restoration of Ras-Erk signaling did not require activation of PI(3)K. Moreover, we found that CD28 signaling induced actin remodeling and polarization of the cortical actin cytoskeleton in thymocytes after inhibition of Csk^{AS}. Whether the function of costimulation via CD28 is to provide a qualitatively different input to complement TCR signals or to quantitatively enhance TCR signal strength has remained an open question. Our data have provided evidence in support of the idea that costimulation via CD28 delivers a unique signal for remodeling of the actin cytoskeleton that is required for the initiation of complete TCR signaling in thymocytes. Surface expression of CD28 is highest on thymocytes; however, the role of CD28 in positive and negative selection in the thymus remains contentious[41–43]. We also cannot fully exclude the possibility that other costimulatory molecules that interact with ligands on thymic

epithelial cells or other cells resident in the thymus provide actin-remodeling signals similar to those provided by CD28.

Finally, we propose the following model for the propagation of TCR signaling in thymocytes: when a thymocyte encounters an APC bearing its cognate pMHC, active Lck initiates a tyrosine-phosphorylation cascade that leads to the phosphorylation and activation of PLC-γ1. Simultaneously, because Lck interacts with and phosphorylates CD28 (ref. 44), the costimulatory CD28-CD80 (or CD28-CD86) interaction delivers local actin-remodeling signals at the site of active TCR signaling. That enables Lat-bound PLC-γ1 to come into sufficient proximity to PtdIns(4,5)P_2, perhaps because the cytoplasmic tail of Lat associated with PLC-γ1 can now access the plasma membrane or because PtdIns(4,5)P_2 is released from binding with the many actin-binding or actin-regulatory proteins it associates with[25,26,37,45]. Alternatively, it has been shown that stimulation of the TCR results in translocation of PLC-γ1 to the cortical actin cytoskeleton[46]. Actin turnover may therefore enhance recruitment of PLC-γ1 to the membrane and thus position it near PtdIns(4,5)P_2. Hydrolysis of PtdIns(4,5)P_2 ensures further propagation of the proximal TCR signal to the calcium and Ras-Erk signaling modules via generation of the critical second messengers Ins(1,4,5)P_3 and diacylglycerol. We suggest that the role of the cortical actin cytoskeleton in regulating the access of signaling enzymes to substrates may apply to other membrane-receptor signaling pathways in other cell types.

METHODS

Methods and any associated references are available in the online version of the paper.

Note: Any Supplementary Information and Source Data files are available in the online version of the paper.

ACKNOWLEDGMENTS

We thank J.A. Bluestone (University of California, San Francisco) for CD80-CD86–deficient mice; J.B. Bolen (Moderna Therapeutics) for the anti-Lck hybridoma; H. Wang (University of California, San Francisco) for anti-ζ; A. Roque and Z. Wang for assisting with animal husbandry and cell sorting, respectively; N. Killeen and Z. Yang for technical assistance with BAC transgenesis; J.S. Shin for technical assistance with isolation of thymic DCs; H. Liu and the University of California, San Francisco Helen Diller Family Comprehensive Cancer Center Mass Spectrometry Core Facility for technical and analytical expertise; and A. DeFranco, C. Lowell and H. Wang for critical reading of the manuscript and discussions. Supported by the Agency for Science, Technology and Research in Singapore (Y.X.T.), the Cancer Research Institute (B.N.M.) and the US National Institutes of Health (PO1 AI091580 to A.W. and 5R01EB001987 to K.M.S.).

AUTHOR CONTRIBUTIONS

Y.X.T. and A.W. designed the research and wrote the manuscript; Y.X.T. did the research and analyzed the data; B.N.M. helped design, do and analyze the immunofluorescence experiments; T.S.F. designed, did and analyzed the data from the *in vitro* kinase assays; C.Z. and K.M.S. designed the Csk^{AS} allele and provided 3-IB-PP1; and all authors commented on the manuscript.

COMPETING FINANCIAL INTERESTS

The authors declare no competing financial interests.

1. Smith-Garvin, J.E., Koretzky, G.A. & Jordan, M.S. T cell activation. *Annu. Rev. Immunol.* **27**, 591–619 (2009).
2. van Oers, N.S., Killeen, N. & Weiss, A. ZAP-70 is constitutively associated with tyrosine-phosphorylated TCR ζ in murine thymocytes and lymph node T cells. *Immunity* **1**, 675–685 (1994).
3. Xu, C. *et al.* Regulation of T cell receptor activation by dynamic membrane binding of the CD3ε cytoplasmic tyrosine-based motif. *Cell* **135**, 702–713 (2008).
4. James, J.R. & Vale, R.D. Biophysical mechanism of T-cell receptor triggering in a reconstituted system. *Nature* **487**, 64–69 (2012).
5. van der Merwe, P.A. & Dushek, O. Mechanisms for T cell receptor triggering. *Nat. Rev. Immunol.* **11**, 47–55 (2011).
6. Palacios, E.H. & Weiss, A. Function of the Src-family kinases, Lck and Fyn, in T-cell development and activation. *Oncogene* **23**, 7990–8000 (2004).
7. Bergman, M. *et al.* The human p50csk tyrosine kinase phosphorylates $p56^{lck}$ at Tyr-505 and down regulates its catalytic activity. *EMBO J.* **11**, 2919–2924 (1992).
8. Hermiston, M.L., Xu, Z., Majeti, R. & Weiss, A. Reciprocal regulation of lymphocyte activation by tyrosine kinases and phosphatases. *J. Clin. Invest.* **109**, 9–14 (2002).
9. Nika, K. *et al.* Constitutively active Lck kinase in T cells drives antigen receptor signal transduction. *Immunity* **32**, 766–777 (2010).
10. Imamoto, A. & Soriano, P. Disruption of the csk gene, encoding a negative regulator of Src family tyrosine kinases, leads to neural tube defects and embryonic lethality in mice. *Cell* **73**, 1117–1124 (1993).
11. Nada, S. *et al.* Constitutive activation of Src family kinases in mouse embryos that lack Csk. *Cell* **73**, 1125–1135 (1993).
12. Schmedt, C. *et al.* Csk controls antigen receptor-mediated development and selection of T-lineage cells. *Nature* **394**, 901–904 (1998).
13. Cloutier, J.F., Chow, L.M. & Veillette, A. Requirement of the SH3 and SH2 domains for the inhibitory function of tyrosine protein kinase $p50^{csk}$ in T lymphocytes. *Mol. Cell. Biol.* **15**, 5937–5944 (1995).
14. Brdicka, T. *et al.* Phosphoprotein associated with glycosphingolipid-enriched microdomains (PAG), a novel ubiquitously expressed transmembrane adaptor protein, binds the protein tyrosine kinase csk and is involved in regulation of T cell activation. *J. Exp. Med.* **191**, 1591–1604 (2000).
15. Davidson, D., Bakinowski, M., Thomas, M.L., Horejsi, V. & Veillette, A. Phosphorylation-dependent regulation of T-cell activation by PAG/Cbp, a lipid raft-associated transmembrane adaptor. *Mol. Cell. Biol.* **23**, 2017–2028 (2003).
16. Kawabuchi, M. *et al.* Transmembrane phosphoprotein Cbp regulates the activities of Src-family tyrosine kinases. *Nature* **404**, 999–1003 (2000).
17. Xavier, R., Brennan, T., Li, Q., McCormack, C. & Seed, B. Membrane compartmentation is required for efficient T cell activation. *Immunity* **8**, 723–732 (1998).
18. Dobenecker, M.W., Schmedt, C., Okada, M. & Tarakhovsky, A. The ubiquitously expressed Csk adaptor protein Cbp is dispensable for embryogenesis and T-cell development and function. *Mol. Cell. Biol.* **25**, 10533–10542 (2005).
19. Xu, S., Huo, J., Tan, J.E. & Lam, K.P. Cbp deficiency alters Csk localization in lipid rafts but does not affect T-cell development. *Mol. Cell. Biol.* **25**, 8486–8495 (2005).
20. Schoenborn, J.R., Tan, Y.X., Zhang, C., Shokat, K.M. & Weiss, A. Feedback circuits monitor and adjust basal Lck-dependent events in T cell receptor signaling. *Sci. Signal.* **4**, ra59 (2011).
21. Gamper, C.J. & Powell, J.D. All PI3Kinase signaling is not mTOR: dissecting mTOR-dependent and independent signaling pathways in T cells. *Front. Immunol.* **3**, 312 (2012).
22. Berridge, M.J. Inositol trisphosphate and calcium signalling mechanisms. *Biochim. Biophys. Acta* **1793**, 933–940 (2009).
23. Kortum, R.L. *et al.* A phospholipase C-γ1-independent, RasGRP1-ERK-dependent pathway drives lymphoproliferative disease in linker for activation of T cells-Y136F mutant mice. *J. Immunol.* **190**, 147–158 (2013).
24. Kusumi, A. *et al.* Paradigm shift of the plasma membrane concept from the two-dimensional continuum fluid to the partitioned fluid: high-speed single-molecule tracking of membrane molecules. *Annu. Rev. Biophys. Biomol. Struct.* **34**, 351–378 (2005).
25. Blin, G. *et al.* Quantitative analysis of the binding of ezrin to large unilamellar vesicles containing phosphatidylinositol 4,5 bisphosphate. *Biophys. J.* **94**, 1021–1033 (2008).
26. Gambhir, A. *et al.* Electrostatic sequestration of PIP2 on phospholipid membranes by basic/aromatic regions of proteins. *Biophys. J.* **86**, 2188–2207 (2004).
27. Treanor, B. *et al.* The membrane skeleton controls diffusion dynamics and signaling through the B cell receptor. *Immunity* **32**, 187–199 (2010).
28. Klein, L., Hinterberger, M., Wirnsberger, G. & Kyewski, B. Antigen presentation in the thymus for positive selection and central tolerance induction. *Nat. Rev. Immunol.* **9**, 833–844 (2009).
29. Proietto, A.I., Lahoud, M.H. & Wu, L. Distinct functional capacities of mouse thymic and splenic dendritic cell populations. *Immunol. Cell Biol.* **86**, 700–708 (2008).
30. Burkhardt, J.K., Carrizosa, E. & Shaffer, M.H. The actin cytoskeleton in T cell activation. *Annu. Rev. Immunol.* **26**, 233–259 (2008).
31. Veillette, A., Bookman, M.A., Horak, E.M. & Bolen, J.B. The CD4 and CD8 T cell surface antigens are associated with the internal membrane tyrosine-protein kinase p56lck. *Cell* **55**, 301–308 (1988).
32. Steinman, R.M. Decisions about dendritic cells: past, present, and future. *Annu. Rev. Immunol.* **30**, 1–22 (2012).
33. Boomer, J.S. & Green, J.M. An enigmatic tail of CD28 signaling. *Cold Spring Harb. Perspect. Biol.* **2**, a002436 (2010).
34. Salazar-Fontana, L.I., Barr, V., Samelson, L.E. & Bierer, B.E. CD28 engagement promotes actin polymerization through the activation of the small Rho GTPase Cdc42 in human T cells. *J. Immunol.* **171**, 2225–2232 (2003).
35. Liang, Y. *et al.* The lymphoid lineage-specific actin-uncapping protein Rltpr is essential for costimulation via CD28 and the development of regulatory T cells. *Nat. Immunol.* **14**, 858–866 (2013).
36. Abraham, R.T. & Weiss, A. Jurkat T cells and development of the T-cell receptor signalling paradigm. *Nat. Rev. Immunol.* **4**, 301–308 (2004).

37. Saarikangas, J., Zhao, H. & Lappalainen, P. Regulation of the actin cytoskeleton-plasma membrane interplay by phosphoinositides. *Physiol. Rev.* **90**, 259–289 (2010).
38. Valitutti, S., Dessing, M., Aktories, K., Gallati, H. & Lanzavecchia, A. Sustained signaling leading to T cell activation results from prolonged T cell receptor occupancy. Role of T cell actin cytoskeleton. *J. Exp. Med.* **181**, 577–584 (1995).
39. Kraus, M., Alimzhanov, M.B., Rajewsky, N. & Rajewsky, K. Survival of resting mature B lymphocytes depends on BCR signaling via the Igα/β heterodimer. *Cell* **117**, 787–800 (2004).
40. Polic, B., Kunkel, D., Scheffold, A. & Rajewsky, K. How αβ T cells deal with induced TCR α ablation. *Proc. Natl. Acad. Sci. USA* **98**, 8744–8749 (2001).
41. Gross, J.A., Callas, E. & Allison, J.P. Identification and distribution of the costimulatory receptor CD28 in the mouse. *J. Immunol.* **149**, 380–388 (1992).
42. Buhlmann, J.E., Elkin, S.K. & Sharpe, A.H. A role for the B7–1/B7–2:CD28/CTLA-4 pathway during negative selection. *J. Immunol.* **170**, 5421–5428 (2003).
43. Dautigny, N., Le Campion, A. & Lucas, B. Timing and casting for actors of thymic negative selection. *J. Immunol.* **162**, 1294–1302 (1999).
44. Holdorf, A.D. *et al.* Proline residues in CD28 and the Src homology (SH)3 domain of Lck are required for T cell costimulation. *J. Exp. Med.* **190**, 375–384 (1999).
45. van Rheenen, J. *et al.* EGF-induced PIP2 hydrolysis releases and activates cofilin locally in carcinoma cells. *J. Cell Biol.* **179**, 1247–1259 (2007).
46. Patsoukis, N. *et al.* RIAM regulates the cytoskeletal distribution and activation of PLC-γ1 in T cells. *Sci. Signal.* **2**, ra79 (2009).

ONLINE METHODS

Generation of Csk^{AS} mice. BAC RP24-400B5, which contains the region of chromosome 9 with the *Csk* locus, was from BACPAC Resources at the Children's Hospital Oakland Resource Institute. The following modifications were engineered by bacterial recombination–mediated genetic engineering[47]: first, mutation of the sequence encoding the mouse Csk threonine residue at position 266 to sequence encoding glycine; second, deletion on both ends of the BAC to leave chromosome 9 positions 57,602,462–57,676,881 (GRCm38.p1 C57BL/6J assembly); and third, introduction of an in-frame stop codon in exon 2 of *Lman1l*. The modified BAC was injected into fertilized C57BL/6 embryos by the Transgenic and Targeted Mutagenesis Core Facility of the University of California, San Francisco. Transgenic founders were crossed to *Csk*$^{-/-}$ mice[10]. Mice were genotyped with the following PCR primers: transgenic allele, 5′-AATAGGGAAGGGGGAGTTTG-3′ and 5′-CTTGGCCATGTACTCT CC-3′; wild-type allele, 5′-AATAGGGAAGGGGGAGTTTG-3′ and 5′-CTT GGCCATGTACTCTGT-3′.

Mice. Mice used for these studies were 4–12 weeks of age. *H2-Ab1*$^{-/-}$*B2m*$^{-/-}$ mice deficient in MHC class I and MHC class II were from Taconic. *Icam1*$^{-/-}$ mice and *Cd80*$^{-/-}$*Cd86*$^{-/-}$ mice have been described[48,49]. All mice were housed in a specific pathogen–free facility at the University of California, San Francisco according to guidelines of the University Animal Care Committee and the US National Institutes of Health.

Inhibitors. 3-IB-PP1 has been described[20] and was used at a concentration of 10 μM. Cytochalasin D, latrunculin A and jasplakinolide (Sigma) were used at concentrations of 10 μM, 0.5 μM and 1 μM, respectively.

Antibodies and reagents. Peridinin chlorophyll protein–cyanin 5.5–anti-CD3 (551163), Alexa Fluor 647–anti-CD3 (557869), peridinin chlorophyll protein–cyanin 5.5–anti-CD4 (550954), phycoerythrin–anti-CD4 (553730), fluorescein isothiocyanate–anti-CD5 (553021), phycoerythrin–indotricarbocyanine–anti-CD8 (552877), phycoerythrin–anti-CD11b (553311), phycoerythrin–anti-CD11c (553802), peridinin chlorophyll protein–cyanin 5.5–anti-CD25 (551071), fluorescein isothiocyanate–anti-CD44 (553133), phycoerythrin–indotricarbocyanine–anti-CD69 (552879), allophycocyanin–anti-CD90.2 (553007), Alexa Fluor 647–anti-B220 (557683), phycoerythrin–anti–γδ TCR (553178), phycoerythrin–anti-NK1.1 (553165) and phycoerythrin–anti-Gr-1 (553128) were from BD Biosciences; fluorescein isothiocyanate–Alexa Fluor 647–anti-CD8 (YTS169.4) was from the monoclonal antibodies core facility of the University of California, San Francisco; phycoerythrin–anti-CD19 (eBioscience 12-0193-83), Alexa Fluor 647–anti-Siglec H (Biolegend 129608); antibody to the mitogen-activated protein kinase p44/42 phosphorylated at TyrThr202 and Tyr204 (4377), antibody to Src phosphorylated at Tyr416 (2101), antibody to Zap70 phosphorylated at Tyr319 (2701; used in **Fig. 1e**), antibody to Lat phosphorylated at Tyr191 (44-228; used in **Supplementary Fig. 3e**), anti-Lat (9166), antibody to Akt phosphorylated at Ser473 (4058) were from Cell Signaling; antibody to Lat phosphorylated at Tyr132 (44-224), antibody to PLC-γ1 (44-696G) and Alexa Fluor 488–anti-phalloidin (A12379) were from Life Technologies; anti-Csk (C20) was from Santa Cruz; antibody to phosphorylated tyrosine (4G10) was from Upstate; antibody to PLC-γ1 phosphorylated at Tyr20, (05-163) was from Millipore; anti-actin (A2066) was from Sigma Aldrich; monoclonal antibody to Lck (1F6) was produced and purified in-house (Weiss laboratory) by standard methods from a hybridoma originally obtained from J.B. Bolen; anti-ζ (H146) was from H. Wang; anti-CD3ε (2C11) and anti-Zap70 (1E7.2) hybridomas were grown, and the monoclonal antibodies were produced and purified in-house (Weiss laboratory) by standard methods; antibody to Lck phosphorylated at Tyr505 (612390) was from BD Biosciences; goat antibody to Armenian hamster immunoglobulin G (IgG) (heavy and light chains) (127-005-160) and donkey antibody to rabbit IgG conjugated to allophycocyanin (711-136-152) were from Jackson Immunoresearch; horseradish peroxidase–conjugated goat antibody to rabbit IgG (heavy and light chains) (4050-05) and mouse IgG (heavy and light chains) (1031-50) and rabbit antibody to hamster IgG (heavy and light chains) (6215-05) were from Southern Biotech; anti-B7.2–immunoglobulin (741-B2-100) was from R&D Systems.

Flow cytometry and data analysis. Stained cells were analyzed on a Fortessa (BD Biosciences). Data were analyzed with FlowJo software (TreeStar).

Cell stimulation and intracellular flow cytometry with phosphorylation-specific antibodies. Before being stimulated, cells were deprived of serum for at least 15 min at 37 °C. Cells were stimulated in serum-free RPMI medium at 37 °C. Crosslinking of CD3ε was induced by the addition of 20 μg/ml anti-CD3ε, followed by goat antibody to Armenian hamster IgG (heavy and light chains) to a final concentration of 50 μg/ml. For bead-based stimulation, 4.5-μm styrene beads (Polyscience) were coated overnight under continuous rotation at 4 °C with B7.2–immunoglobulin (5 μg/ml) and/or I-A^b tetramer loaded with human MHC class II–associated invariant chain peptide 103-117 (5 μg/ml; tetramer core facility of the US National Institutes of Health) in PBS. Beads were then saturated with 1% BSA in PBS under continuous rotation for at least 1 h at 25 °C, and were washed with PBS before use. Intracellular staining of phosphorylated Erk and Akt was done as described[20].

Calcium-flux assay. Cells were loaded for 30 min at 37 °C with the fluorescent Ca^{2+} indicator dye Indo 1–AM (1.5 μM; Invitrogen) in RPMI medium with 5% FBS and washed, then their surfaces were stained and cells were kept on ice in 5% FBS in RPMI medium. Cells were warmed to 37 °C for 5 min before stimulation.

Immunoblot analysis and immunoprecipitation. Cells were lysed directly in 6× SDS-PAGE sample buffer after stimulation. Proteins were separated by SDS-PAGE and transferred to Immobilon-P polyvinylidene difluoride membranes (Millipore) by standard immunoblot technique, and were visualized with SuperSignal ECL reagent or SuperSignal West Femto maximum sensitivity substrate (Pierce Biotechnology) on a Kodak Imaging Station. For immunoprecipitation, cells were lysed in 1% NP-40 lysis buffer with inhibitors of proteases and phosphatases, and lysates were incubated overnight at 4 °C with protein G–Sepharose beads preincubated with anti-ζ. Immunoprecipitates were washed three times with 1 ml lysis buffer before elution from beads.

Microscopy. Cell-bead conjugates were fixed for 30 min at 25 °C in 4% paraformaldehyde and 0.2% glutaraldehyde. After 'spin washes' in PBS and staining buffer (2% FCS in PBS), cells were permeabilized for 5 min in 0.05% Triton X-100 and washed with staining buffer. After 30 min in staining buffer, conjugates were stained with allophycocyanin–anti-CD90.2 (553007; BD Biosciences) and phalloidin–Alexa Fluor 488 (A12379; Life Technologies). The *z*-stacks of conjugates were imaged unmounted in Ibidi 96-well plates with 40× air objective on Zeiss Axiovert 200M. The best focus of the cell-bead interface was assigned scores for polarization of F-actin toward beads, with masking of the identity of the stimulus.

Cell enrichment. Enriched populations of CD4$^+$ T cells or 'pan–T cells' were obtained by negative selection according to the manufacturer's protocol (19752 and 19751; Stemcell Technologies). Enriched populations of DCs were obtained by CD11c$^+$ selection according to the manufacturer's protocol (18758 or 18780; Stemcell Technologies). Thymic DCs were obtained by grinding of the thymus in gentleMACS C tubes (Miltenyi Biotec) with the Spleen 2 program, followed by digestion for 20 min at 37 °C with 62.4 μg/ml DNaseI (Roche) and 1.25 mg/ml collagenase D (Worthington), then further grinding with the Spleen 1 program. The single-cell suspension obtained was stained on the surface and then sorted for CD11c$^+$ cells after 'dumping' of B220^{hi}, CD3^{hi}, Siglec H–high and side scatter–high cells.

Measurement of total inositol phosphates. Thymocytes (4×10^7 cells per ml) were labeled for 6 h at 37 °C with 40 μCi/ml of [^{3}H]-myo-inositol (Perkin Elmer), then were washed and were cultured overnight at 37 °C in RPMI medium containing 10% fetal bovine serum, 10 mM HEPES, 2 mM L-glutamine, 55 μM β-mercaptoethanol, 0.11 mg/ml sodium pyruvate, non-essential amino acids, 100 units penicillin and 0.1 mg/ml streptomycin. Labeled thymocytes were treated for 20 min at 37 °C with 20 mM lithium chloride and stimulated. Cells were lysed in 0.75 ml of chloroform–methanol–12 M hydrochloric acid (100:200:2) and the phases were separated by the addition of 0.25 ml H_2O and 0.25 ml chloroform. The upper aqueous phase was mixed

with 2.3 ml H_2O and the precipitate formed was pelleted. The aqueous phase was then applied to columns made from 1.2 ml of a 0.5-g/ml aqueous slurry of AG 1-X8 (Biorad 140-1444). [^{3}H]inositol and [^{3}H]glycerophosphorylinositol were washed off with 18 ml of a 60-mM solution of sodium formate–5 mM disodium tetraborate. Total inositol phosphates were eluted with 10 ml of 1 M ammonium formate plus 0.1 M formic acid. Radioactivity was determined by scintillation counting in Ecoscint (National Diagnostics).

Protein purification. cDNA encoding full-length mouse Csk, the PP1 analog–sensitive mutant T266G (Csk^{AS}) or the mutant K222R with kinase impairment (Csk^{K222R})[50] was subcloned into pGEX-6P-3 vector containing an amino-terminal glutathione *S*-transferase (GST) affinity tag. Each vector was transformed into BL21(DE3) cells (Agilent), and expression was induced overnight at 18 °C with 0.2 mM isopropyl-β-D-thio-galactoside (IPTG). The bacterial pellet was resuspended in GST binding buffer, pH 7.4 (5 mM EDTA and 5 mM dithiothreitol (DTT) in PBS) and was lysed by freezing and thawing, lysozyme treatment and sonication (Branson 450). All purification steps were done on ice or at 4 °C, and all columns and proteases were from GE Healthcare. The clarified lysate was affinity-purified by being bound to a GST Gravitrap column, followed by elution at a pH of 8.0 with 10 mM reduced glutathione, 25 mM Tris, 50 mM NaCl and 1 mM DTT. The GST tag was cleaved overnight with PreScission Protease. After buffer exchange by concentration and dilution, Csk was further purified by HiTrap Q anion-exchange chromatography at a pH of 8.0 (50 mM Tris, 50–1,000 mM NaCl and 1 mM DTT), followed by a Superdex 200 gel filtration column in 100 mM NaCl, 10% glycerol and 50 mM Tris, pH 8.0. Purified Csk was flash-frozen in liquid nitrogen and was stored at −70 °C. Homogeneity and molecular weight of purified proteins were verified by SDS-PAGE and mass spectrometry. The concentration of purified Csk was determined from its absorbance at 280 nm with a molar absorption of 73800 M^{-1} cm^{-1} calculated with the ExPASy ProtParam tool for the computation of the physical and chemical parameters of a protein[51].

Kinase activity assay. The activity of purified Csk was obtained from a continuous spectrometric assay in which hydrolysis of ATP is coupled via pyruvate kinase and lactate dehydrogenase to NADH oxidation, which results in a decrease in absorbance at 340 nm (ref. 52). Kinase activity was measured at 30 °C with a Molecular Devices Spectramax 340PC spectrophotometer in a reaction volume of 75 µl with final concentrations of 2.5 µM Csk, 55.7 U/ml pyruvate kinase, 78 U/ml lactate dehydrogenase, 0.6 mg/ml NADH, 1 mM phosphoenolpyruvate, 250 µM ATP, 10 mM Tris, pH 7.5, 1 mM $MgCl_2$, and 1 mM Tris(2-carboxyethyl)phosphine (TCEP). The reaction was initiated by the addition of the Csk optimal peptide substrate (KKKKEEIYFFF[53]) at a final concentration of 250 µM (synthesized by Elim Biosciences). Negligible background activity was observed if the substrate or kinase was omitted from the reaction. Kinase activity was obtained by fitting of the initial segment of the decay curve to a linear function. For curves measuring the median inhibitory concentration (IC_{50}), independent samples were mixed with DMSO (dimethylsulfoxide) containing varying concentrations of 3-IB-PP1 just before the initiation of the reaction. Linear velocities were obtained at each concentration of 3-IB-PP1 and were normalized between 0% and 100% in each data set. Data sets were fit globally to the function $y = 100/(1 + 10^{x - \log IC_{50}})$ to determine the IC_{50} value. GraphPad Prism software was used for all curve fitting and statistical analysis.

Statistical analysis. Microsoft Excel was used for statistical analyses with paired *t*-tests. Sample-size choice and assumption of normality were based on similar analyses in published studies.

47. Tischer, B.K., von Einem, J., Kaufer, B. & Osterrieder, N. Two-step red-mediated recombination for versatile high-efficiency markerless DNA manipulation in *Escherichia coli*. *Biotechniques* **40**, 191–197 (2006).
48. Sligh, J.E. Jr. *et al*. Inflammatory and immune responses are impaired in mice deficient in intercellular adhesion molecule 1. *Proc. Natl. Acad. Sci. USA* **90**, 8529–8533 (1993).
49. Borriello, F. *et al*. B7–1 and B7–2 have overlapping, critical roles in immunoglobulin class switching and germinal center formation. *Immunity* **6**, 303–313 (1997).
50. Chow, L.M., Fournel, M., Davidson, D. & Veillette, A. Negative regulation of T-cell receptor signalling by tyrosine protein kinase $p50^{csk}$. *Nature* **365**, 156–160 (1993).
51. Gasteiger, E. *et al*. Protein identification and analysis tools on the ExPASy server. in *The Proteomics Protocols Handbook* (ed. Walker, J.M.) 571–607 (Humana, 2005).
52. Barker, S.C. *et al*. Characterization of pp60c-src tyrosine kinase activities using a continuous assay: autoactivation of the enzyme is an intermolecular autophosphorylation process. *Biochemistry* **34**, 14843–14851 (1995).
53. Sondhi, D., Xu, W., Songyang, Z., Eck, M.J. & Cole, P.A. Peptide and protein phosphorylation by protein tyrosine kinase Csk: insights into specificity and mechanism. *Biochemistry* **37**, 165–172 (1998).

doi:10.1038/ni.2772

Supplementary Information for

Inhibition of Csk in thymocytes reveals a requirement for actin remodeling in the initiation of full T cell receptor signaling

Ying Xim Tan[1], Boryana N. Manz[1], Tanya Freedman[1], Chao Zhang[3], Kevan M. Shokat[4,5], Arthur Weiss[1,2,5*]

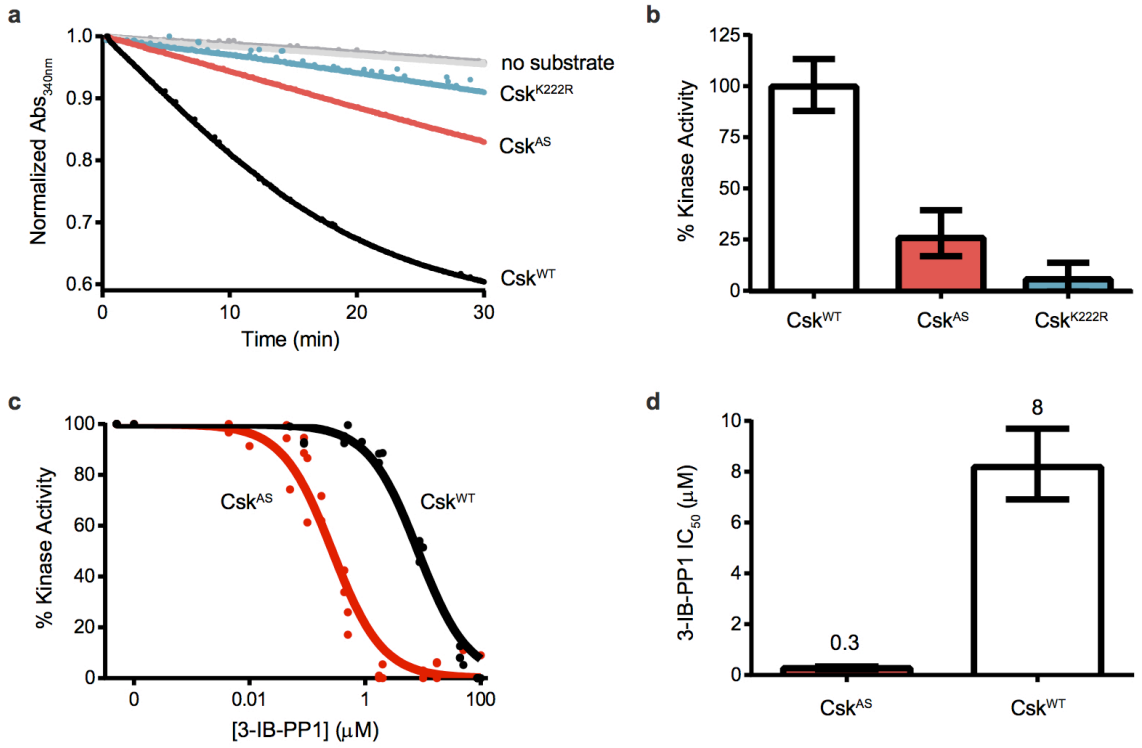

Supplementary Figure 1. The Csk^{AS} allele is active and can be specifically inhibited by the PP1 analog, 3-IB-PP1. (**a**) Substituting glycine for threonine at the gatekeeper position in the active site of Csk to generate analog sensitive Csk (Csk^{AS}) impairs but does not abrogate kinase activity in purified Csk^{AS}, as monitored by decreasing absorbance in an assay coupling ATP hydrolysis to NADH oxidation. (**b**) Csk^{AS} phosphorylates peptide at a rate in between that of Csk^{WT} and the kinase-impaired variant Csk^{K222R}. Error bars represent 95% confidence intervals (CI), n=4. The Csk variants are significantly different from each other ($p<0.0001$) in a one-way ANOVA test (or $p=0.0041$ (Csk^{AS}, Csk^{K222R}) in a two-tailed t test). (**c**) A bulky analog of kinase inhibitor PP1, 3-IB-PP1, specifically targets Csk^{AS} over Csk^{WT}. Data points are independent samples from four (Csk^{WT}) or five (Csk^{AS}) separate experiments, and lines represent fit dose-response curves. (**d**) 3-IB-PP1 has a 27-fold lower IC_{50} for Csk^{AS} than for Csk^{WT}. Error bars represent 95% CI of a global fit.

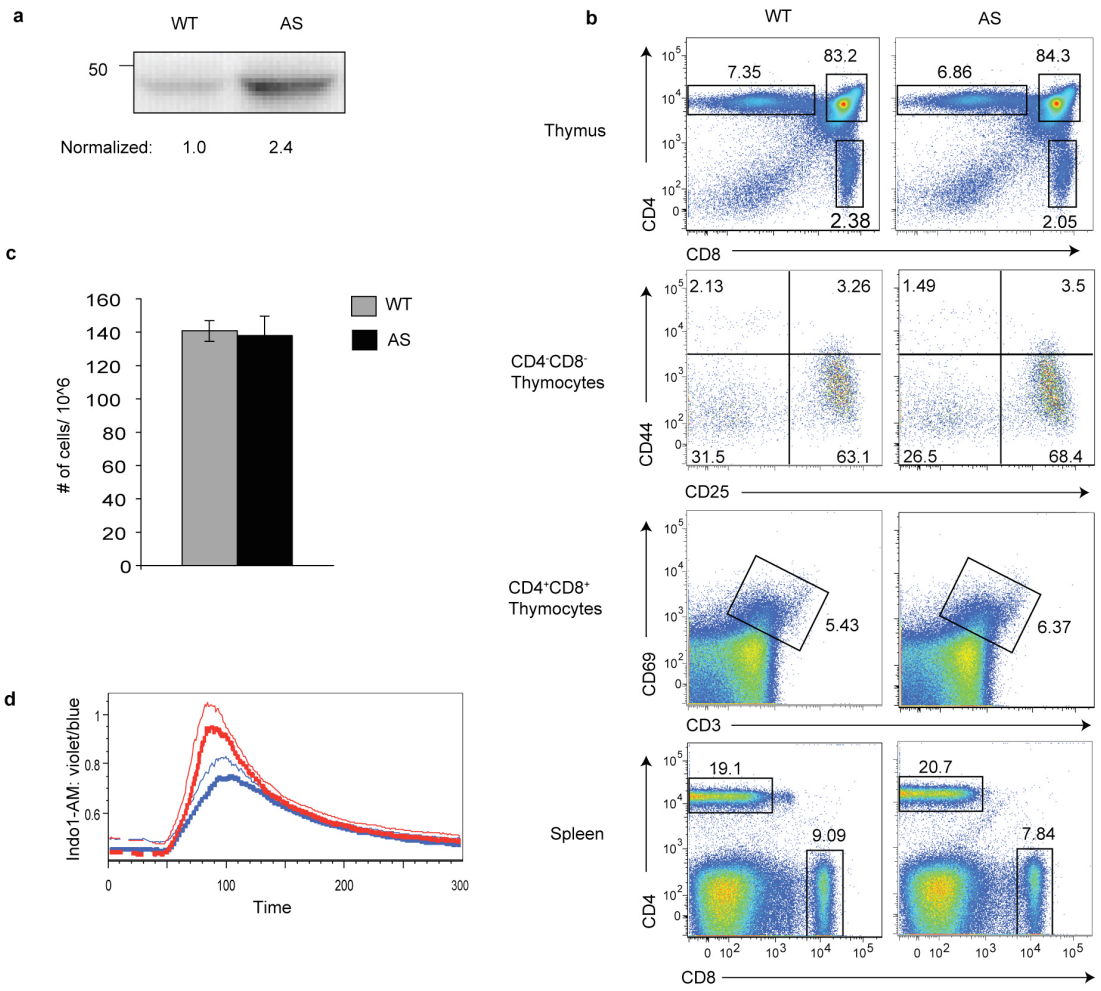

Supplementary Figure 2. T cell develop normally and respond normally to TCR stimulation in Csk^{AS} BAC transgenic mice. (**a**) Immunoblot and densitometric analysis of Csk expression in wild-type (WT) and Csk^{AS}(AS) thymocytes. (**b**) Thymocytes or splenocytes from wild-type (WT) and Csk^{AS}(AS) thymi were surface stained for the indicated markers and analyzed by flow cytometry. Data representative of five littermate pairs. (**c**) Mean thymic cellularity of ten wild-type (WT) and ten Csk^{AS}(AS) littermate thymi with means and S.E.M indicated. (**d**) Thymocytes from wild-type (WT:thin lines) or Csk^{AS} (AS:thick lines) mice loaded with Indo-1AM dye were stimulated with high dose (red lines: 20μg/mL) or low dose (blue lines: 5μg/mL) anti-CD3ε. Ratiometric assessment of intracellular calcium of CD4^{+}CD8^{+} thymocytes over time is shown. Data is representative of three independent experiments.

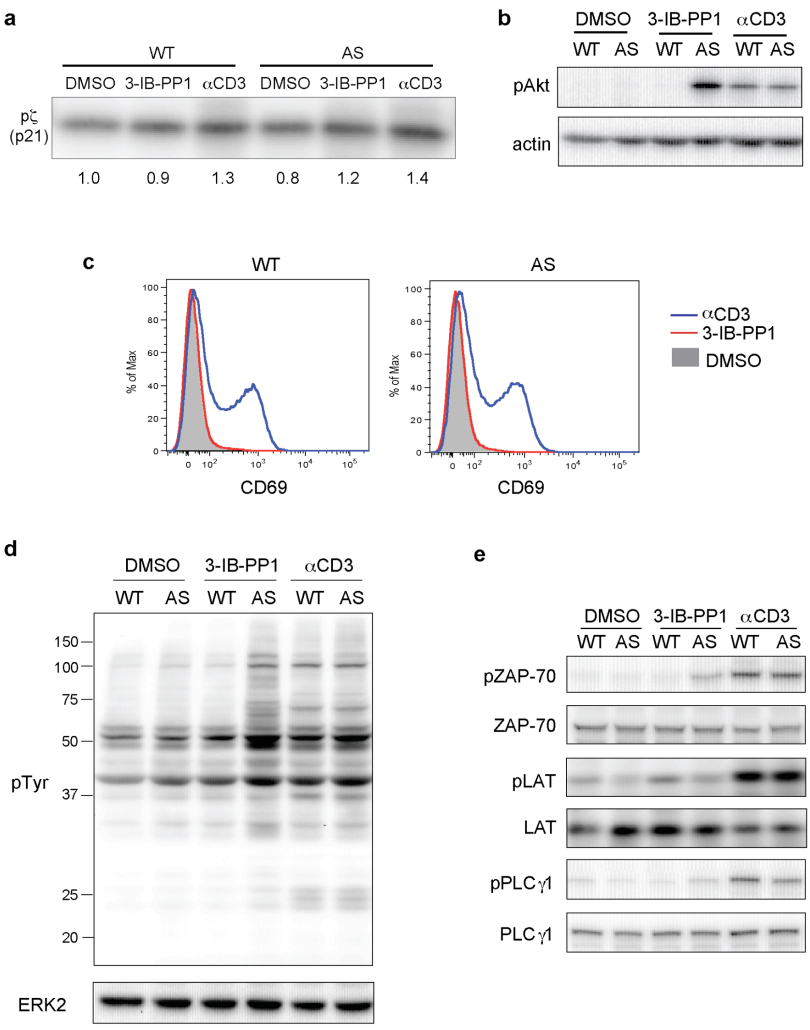

Supplementary Figure 3. Inhibition of Csk^{AS} induces tyrosine phosphorylation but not CD69 upregulation in primary murine T cells. (**a**) Lighter exposure of pTyr blot from Figure 1d with quantification of p21 normalized to total ζ immunoprecipitated. (**b**) Thymocytes from wild-type (WT) or Csk^{AS} (AS) mice were treated for 3min with DMSO, 10 μM 3-IB-PP1 and 20 μg/mL anti-CD3ε then lysed and analyzed by immunoblot with the indicated antibodies. (**c**) Thymocytes from wild-type (WT) or Csk^{AS} (AS) mice were treated with DMSO, 10 μM 3-IB-PP1 or 10 μg/mL platebound anti-CD3ε for 12 hours, stained for cell surface CD69 and analyzed by flow cytometry. Histograms are gated on $CD4^{+}CD8^{+}$ thymocytes. (**d, e**) Purified peripheral $CD4^{+}$ T cells from wild-type (WT) or Csk^{AS} (AS) mice were treated for 3min as indicated, then lysed and analyzed by immunoblot with the indicated antibodies. (**a-c and e**) Data is representative of three independent experiments. (**d**) Data is representative of 2 independent experiments.

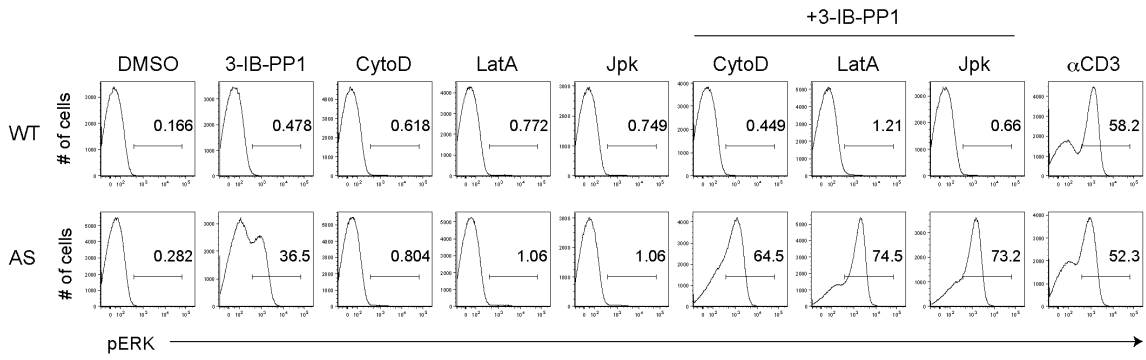

Supplementary Figure 4. Simultaneous alteration of the actin cytoskeleton enhances Erk phosphorylation in thymocytes during inhibition of Csk^{AS}. Thymocytes from wild-type (WT) or Csk^{AS} (AS) mice were stimulated for 2 min as indicated (10 μM 3-IB-PP1; CytoD, 10 μM cytochalasin D; LatA, 0.5 μM latrunculin A; Jpk, 1 μM jasplakinolide; 20 μg/mL anti-CD3ε), then analyzed for pErk content by phosphoflow. Histograms are gated on $CD4^+CD8^+$ thymocytes. Data is representative of two independent experiments. Numbers within histograms indicate percentage of $pErk^+$ cells.

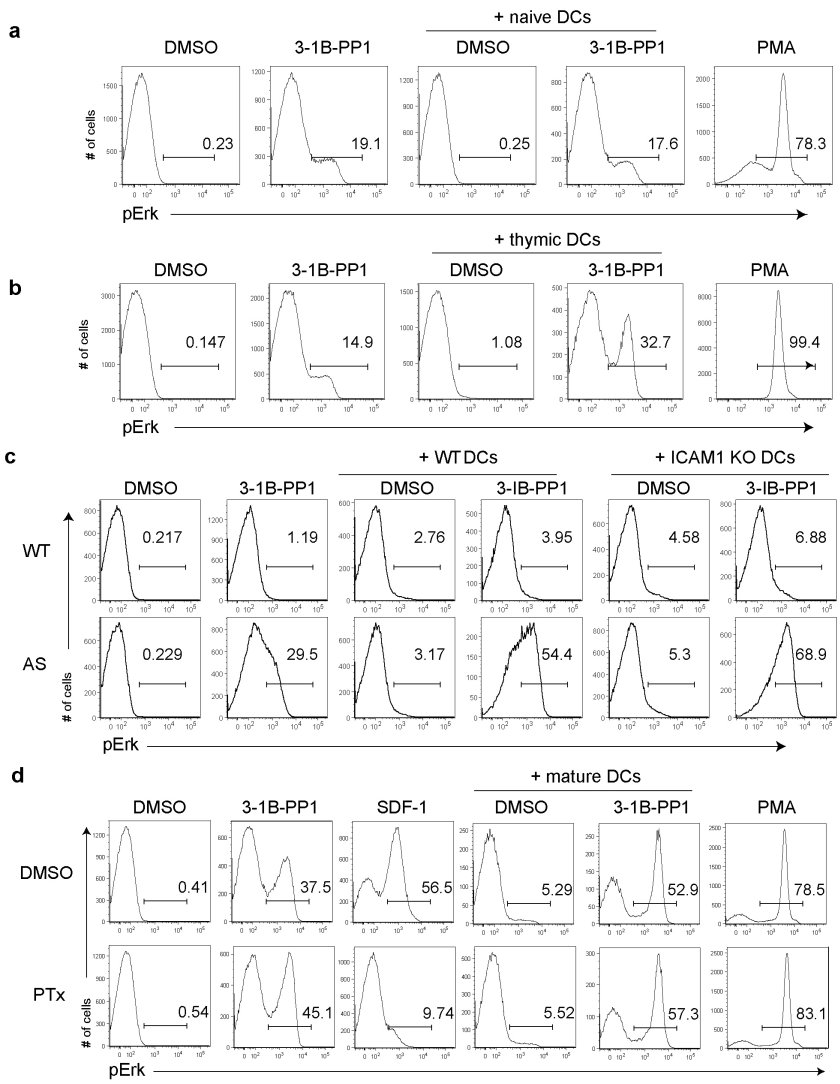

Supplementary Figure 5. Thymic DCs, but not naïve splenic DCs, ICAM-1 deficient DCs or chemokines secreted by mature splenic DCs, enhance ERK phosphorylation in thymocytes during Csk^{AS} inhibition. (**a**) Naïve DCs were enriched from wild-type splenocytes by CD11c positive selection and used immediately. Data is representative of two independent experiments. (**b**) Thymic DCs were sorted from wild-type thymi as described in methods. Data is representative of three independent experiments. (**c**) DCs were enriched from ICAM-1 deficient splenocytes and activated by overnight culture. (**d**) Thymocytes from Csk^{AS} mice were treated with DMSO or 50 ng/mL pertussis toxin (PTx) for 1h. Data is representative of two independent experiments. (**a, b** and **d**) Thymocytes from Csk^{AS} mice or (**c**) wild-type (WT) and Csk^{AS} (AS) mice were pelleted with or without DCs at a 1:1 ratio and stimulated with vehicle (DMSO), 10 μM 3-IB-PP1, 10 ng/mL stromal cell-derived factor (SDF-1) or 50 ng/mL phorbol myristate acetate (PMA) for 3min. Cells were then analyzed for pErk content by phosphoflow. Histograms shown are gated on $CD4^+CD8^+$ thymocytes. Numbers within histograms indicate percentage of $pErk^+$ cells.

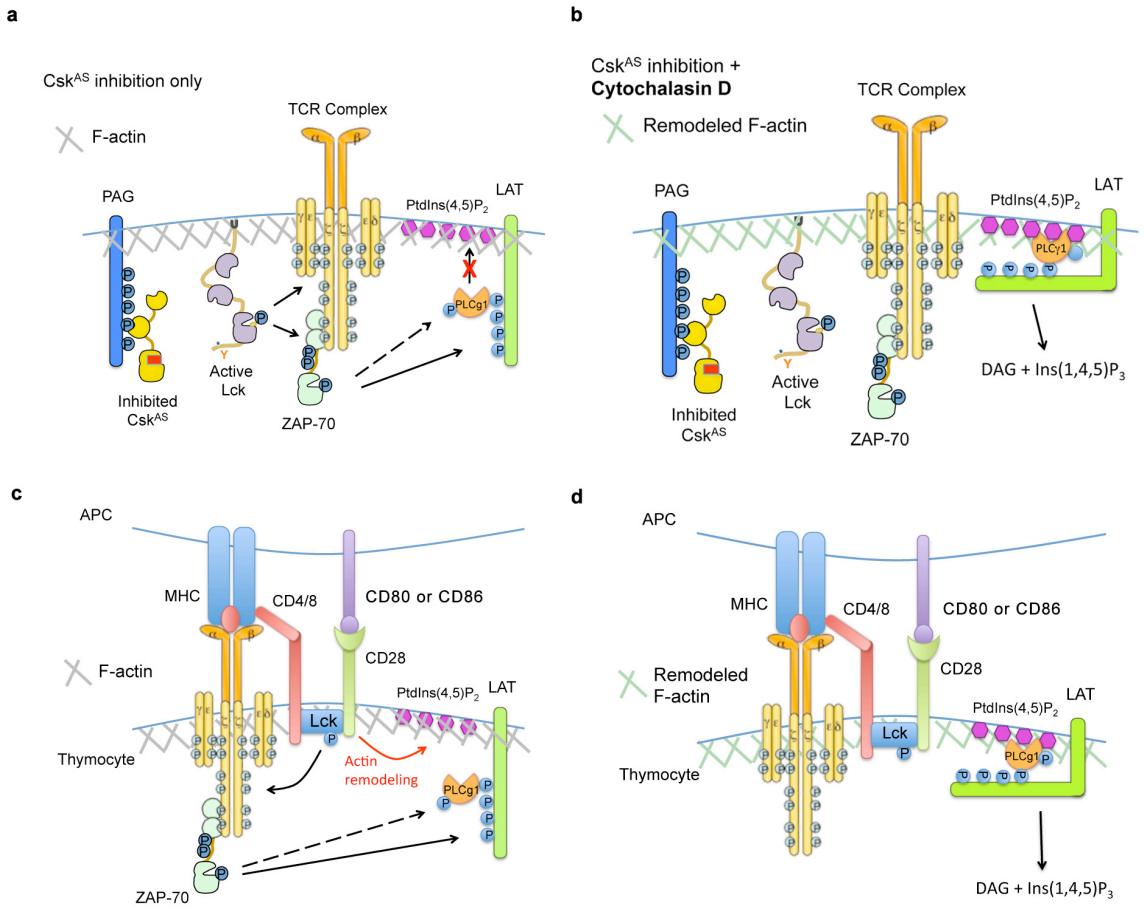

Supplementary Figure 6. Model for TCR signal initiation and propagation in thymocytes. (**a**) Perturbing the Csk-CD45 equilibrium regulating Lck by inhibiting Csk^{AS} results in potent Lck activation, thereby initiating phosphorylation of CD3 and ζ ITAMs and ZAP-70, and eventually activation of PLC-γ1 bound to the LAT signalosome. However, in the absence of actin turnover, active PLC-γ1 cannot access plasma membrane PtdIns(4,5)P_2 to hydrolyze it because the dense cortical actin meshwork and its associated proteins may act as a barrier or because PLC-γ1 fails to be recruited to the actin cytoskeleton. (**b**) Inducing remodeling of the cortical actin cytoskeleton with cytochalasin D allows active PLC-γ1 to access and hydrolyze PtdIns(4,5)P_2 to generate DAG and Ins(1,4,5)P_3. (**c**) During a thymocyte-APC interaction, TCR engagement by pMHC recruits CD4 or CD8 coreceptor bound active Lck. Association of CD80 or CD86 engaged CD28 with Lck allows for activation of local actin cytoskeletal remodeling. (**d**) This enables active PLC-γ1 to hydrolyze PtdIns(4,5)P_2.